American Mineralogist, Volume 95, pages 1527–1532, 2010

Françoisite-(Ce), a new mineral species from La Creusaz uranium deposit (Valais, Switzerland) and from Radium Ridge (Flinders Ranges, South Australia): Description and genesis

NICOLAS MEISSER,[1,*] JOËL BRUGGER,[2,3] STEFAN ANSERMET,[1] PHILIPPE THÉLIN,[4] AND FRANÇOIS BUSSY[5]

[1]Musée de Géologie and Laboratoire des Rayons-X, Institut de Minéralogie et de Géochimie, UNIL, Anthropole, CH-1015 Lausanne-Dorigny, Switzerland
[2]South Australian Museum, North Terrace, 5000 Adelaide, Australia
[3]TRaX, School of Earth and Environmental Sciences, University of Adelaide, 5005 Adelaide, Australia
[4]Laboratoire des Rayons-X, Institut de Minéralogie et de Géochimie, UNIL, Anthropole, CH-1015 Lausanne-Dorigny, Switzerland
[5]Laboratoire de la microsonde électronique, Institut de Minéralogie et de Géochimie, UNIL, Anthropole, CH-1015 Lausanne-Dorigny, Switzerland

ABSTRACT

The new mineral françoisite-(Ce), $(Ce,Nd,Ca)[(UO_2)_3O(OH)(PO_4)_2]\cdot 6H_2O$ is the Ce-analog of françoisite-(Nd). It has been discovered simultaneously at the La Creusaz uranium deposit near Les Marécottes in Valais, Switzerland, and at the Number 2 uranium Workings, Radium Ridge near Mt. Painter, Arkaroola area, Northern Flinders Ranges in South Australia. Françoisite-(Ce) is a uranyl-bearing supergene mineral that results from the alteration under oxidative conditions of REE- and U^{4+}-bearing hypogene minerals: allanite-(Ce), monazite-(Ce), ±uraninite at Les Marécottes; monazite-(Ce), ishikawaite-samarskite, and an unknown primary U-mineral at Radium Ridge. The REE composition of françoisite-(Ce) results from a short aqueous transport of REE leached out of primary minerals [most likely monazite-(Ce) at Radium Ridge and allanite-(Ce) at La Creusaz], with fractionation among REE resulting mainly from aqueous transport, with only limited Ce loss due to oxidation to Ce^{4+} during transport.

Keywords: Françoisite-(Ce), new mineral, rare earth elements, supergene

INTRODUCTION

The phosphate françoisite-(Ce), $(Ce,Nd,Ca)[(UO_2)_3O(OH)(PO_4)_2]\cdot 6H_2O$, is a new mineral species discovered simultaneously at the La Creusaz uranium deposits near Les Marécottes in Valais, Switzerland, and at the Number 2 uranium Workings, Radium Ridge near Mt. Painter, Arkaroola area, Northern Flinders Ranges of South Australia. At the La Creusaz deposit, françoisite-(Ce) was first found in 1981 but analyzed and identified as a new mineral species only in 1999.

Françoisite-(Ce) is the Ce-analog of françoisite-(Nd), a mineral described by Piret et al. (1988) from Kamoto, Shaba, Democratic Republic of Congo (RDC). The new mineral is named françoisite-(Ce) following rule of Levinson (1966) in accordance with the International Mineralogical Association (IMA) recommendations for the nomenclature of rare-earth element (REE)-bearing minerals. The new mineral was approved by the IMA Commission on New Minerals and Mineral Names (vote no. 2004-029). Holotype specimens are deposited at Musée géologique cantonal, Lausanne, Switzerland, under the following catalog numbers: MGL58321 (La Creusaz, Les Marécottes, Valais, Switzerland) and MGL79288 (Number 2 Workings, Radium Ridge, Arkaroola, South Australia). Due to the abundance and quality of crystals found at La Creusaz, most analyses were performed on material from this locality.

* E-mail: nicolas.meisser@unil.ch

OCCURRENCES AND GEOLOGICAL SETTINGS

At both localities (La Creusaz and Radium Ridge), françoisite-(Ce) forms part of a varied assemblage of uranyl-bearing minerals resulting from the alteration of a primary uranium (±REE) mineralization. However, the metallogenesis, geochemical, and mineralogical characters of both occurrences are very different, as summarized below.

La Creusaz uranium prospect

Françoisite-(Ce) was found in the "Gisiger" surface scratching (~630 m^2) at the La Creusaz uranium prospect near the village of "Les Marécottes" (canton Valais, Western Alps, Switzerland; Swiss federal coordinates: 566.208/107.809; altitude 1642 m). The uranium deposit of La Creusaz was discovered in 1973 (Gilliéron 1988), and explored episodically between 1973 and 2008 using drill holes, surface scratching, and galleries.

The mineralization occurs in hydrothermal breccia veins at the contact between the pre-Variscan gneissic basement of the Aiguilles Rouges Massif and the Carboniferous (Variscan) Vallorcine granite. According to Meisser (2003), the complex mineral assemblages and ore textures found at La Creusaz result from a complex geological history.

(1) The primary mineralization event (probably Permo-Triassic) resulted in the precipitation of uraninite and pyrite in breccia and veins. A second, later mineralization stage is characterized by intense brecciation and silicification with precipitation of minor amounts of siderite, chalcopyrite, sphalerite, Se-bearing

galena, and laitakarite [$Bi_4(Se,S)_3$]. Laitakarite gave a Pb/Pb age of 239 ± 7 My (Triassic).

(2) The ores were partially remobilized during the Tertiary Alpine metamorphism under lowest Greenschist facies conditions. Locally intense fluid circulation led to the formation of the rare minerals wittite [$Pb_3Bi_4(S,Se)_9$] and Se-rich weibullite [$Pb_5Bi_8(Se,S)_{18}$] by sulfidation of laitakarite. In late-stage Alpine vugs (~2.5 kbar and 350 °C), well-shaped Dauphiné habit quartz crystals coexist with albite, abundant clinochlore ± chamosite, coffinite, arsenopyrite, chalcopyrite, minor Ag-poor lillianite ($Ag_xPb_{3-3x}Bi_{2+2x}S_6$, with x = 0.12), Se-poor galena, anatase, and titanite.

(3) Strong mechanical and chemical weathering occurred during the Quaternary, especially at the beginning of the interglacial Riss-Wurm period. At this time, the melting of the ice sheet produced rapid decompression, uplift, and fracturing of the rocks, followed by intense fluid circulation. The oxidation of pyrite and arsenopyrite produced acidic fluids, which reacted with uraninite, fluorapatite, and silicates from the host rock. This resulted in the formation of a complex assemblage of uranyl-bearing minerals at La Creusaz, characterized by the coexistence of silicates, oxyhydroxides, arsenates, phosphates, and selenites. This event is dated at ~140 000 years using the ^{238}U-^{234}U-^{230}Th disequilibrium method applied to the abundant uranophane characteristic of this weathering stage. The new mineral species described here, françoisite-(Ce), crystallized during this stage.

(4) Since the end of the underground exploration in 1981, exposed veins and stockpiled U ore have been subjected to acid mine drainage water and atmospheric oxygen in the abandoned galleries. Oxidation of the sulfides (mainly pyrite and chalcopyrite) in the presence of strong bacterial activity resulted in the production of acid (pH ~ 3.1), sulfate-rich waters. These waters reacted with uraninite, clinochlore, illite, calcite, and siderite to form a rich assemblage of neoformed uranyl minerals, including the new minerals marécottite $Mg_3(UO_2)_8(SO_4)_4O_6(OH)_2 \cdot 28H_2O$ (Brugger et al. 2003a) and pseudojohannite $Cu_5(UO_2)_6(SO_4)_3(OH)_{16} \cdot 14H_2O$ (Brugger et al. 2006b), as well as jáchymovite $(UO_2)(SO_4)(OH)_{14} \cdot 13H_2O$, johannite $Cu(UO_2)_2(SO_4)_2(OH)_2 \cdot 8H_2O$, magnesiozippeite $Mg(UO_2)_2(SO_4)O_2 \cdot 3.5H_2O$, natrozippeite $Na(UO_2)_2(SO_4)O(OH) \cdot 2H_2O$, rabejacite $Ca(UO_2)_4(SO_4)_2(OH)_6 \cdot 6H_2O$, schoepite $(UO_2)_8O_2(OH)_{12} \cdot 12H_2O$, schröckingerite $NaCa_3(UO_2)(CO_3)_3(SO_4)F \cdot 10H_2O$, uranopilite $(UO_2)_6(SO_4)(OH)_{10} \cdot 12H_2O$, zippeite $K(UO_2)_2(SO_4)O(OH) \cdot 2H_2O$, and an unnamed Al-equivalent of coconinoite $Al_4(UO_2)_2(PO_4)_4(SO_4)(OH)_2 \cdot 20H_2O$.

At La Creusaz, françoisite-(Ce) is directly associated with abundant uranophane, nováčekite-metanováčekite, jarosite and minor françoisite-(Nd), metatorbernite, metazeunerite, arsenuranospathite, uranospathite, and hyalite. Primary allanite-(Ce), monazite-(Ce), and fluorapatite are locally abundant as accessory minerals in various gneisses that serve as a matrix for specimen of the new mineral.

Number 2 Workings, Radium Ridge

The Number 2 Workings, located on Radium Ridge near Mt. Painter, near Arkaroola, Northern Flinders Ranges, South Australia (Australian Grid coordinates: 54J 0339200mE, 6655430mN), are part of several uranium prospects discovered in 1906 and exploited episodically for radium from 1906–1934 (Brugger et al. 2003b; Coats and Blissett 1971). The workings are located in the Mesoproterozoic Mt. Painter Inlier in the Northern Flinders Ranges, South Australia (Drexel et al. 1993; Fanning et al. 2003). The Mt. Painter Inlier contains large volumes of granites and gneisses highly enriched in U and Th (several tens of parts per million). The radiogenic heat released by these granites is responsible for a long-lasting thermal anomaly (e.g., Sandiford et al. 1998; Neumann et al. 2000), which resulted in large-scale hydrothermal activity within and around the Mt. Painter area. Small-scale on-going hydrothermal activity—probably limited by the low precipitation levels since the last ice age—is documented by the Paralana Hot Springs (Brugger et al. 2005).

The province contains many small Paleozoic hematite-U-Cu-Nb-REE deposits, and a large epithermal system characterized by complex quartz±fluorite veins and breccias (Coats and Blissett 1971; Drexel and Major 1990; Elburg et al. 2003). The Number 2 Workings explored a small (~4 × 4 m) lens of coarse hematite-quartz ore; the other primary minerals include monazite-(Ce), xenotime-(Y), a solid solution between ishikawaite and Fe-rich samarskite, an unidentified Ca-Fe-phosphate, and an unidentified U(Pb,Mn)-oxide primary mineral always fully replaced by a complex assemblage of secondary minerals (mainly metaschoepite and a Mn-Pb oxide, probably cesarolite). The phosphate-REE mineralization can constitute >50 vol% of the ore locally. This Fe-U-Cu-Nb-REE mineralization is overprinted by the epithermal mineralization, consisting of quartz veins with abundant pseudomorphs after fluorite and "needle quartz" growing around (now usually dissolved) acicular crystals of laumontite. A similar evolution from magmatic hydrothermal conditions (510 ± 20 °C) to epithermal (100–140 °C) was described by Bakker and Elburg (2006) from unusual diopside-titanite veins located ~3 km SSE of the Number 2 Workings. A distinct geochemical relationship between the hematite lens at Number 2 and the titanite-diposide veins is indicated by the presence of Nb-rich inclusions in the titanite, as well as abundant fluorapatite (Bakker and Elburg 2006). The titanite was dated at 440 Ma at the time of intrusion of the British Empire Granite (Elburg et al. 2003), but paleomagnetic data suggest that at least two major hydrothermal events affected the Mt. Painter area in the Permo-Carboniferous (Idnurm and Heinrich 1993).

At the Number 2 Workings, secondary uranium minerals occur mainly in the cavities of the epithermal quartz, and in cavities resulting from the dissolution of the unknown primary U-(Pb,Mn)-oxide mineral. Françoisite-(Ce) was found in the latter location. Françoisite-(Ce) from Number 2 Workings is directly associated with metatorbernite, barite, an abundant kaolinite-group mineral, and cesarolite(?). Other secondary minerals reported at Number 2 Workings include curite, billietite, boltwoodite, hyalite, kasolite, rutherfordine, schoepite, and metaschoepite, soddyite, spriggite, meta-torbernite, uranophane-β, weeksite, and the new mineral IMA no. 2008-022: monoclinic-$UO_2(OH)_2$ (Brugger et al. 2003b, 2004).

Appearance and physical properties

At the Number 2 Workings, françoisite-(Ce) forms scale-shaped crystals up to 1 mm in size; X-ray diffraction reveals that the crystals are mixed with microscopic inclusions of a kaolinite-group mineral. Consequently, physical properties

for françoisite-(Ce) were measured on the more abundant and pure material from La Creusaz. At La Creusaz, françoisite-(Ce) forms radial aggregates constituted of lemon yellow prismatic crystals elongated along [001] and measuring up to ~100 μm in length (Fig. 1), growing directly in gneisses adjacent to the uraninite-bearing hydrothermal breccia. Crystals are transparent, with a vitreous luster and a pale yellow ("Naples yellow") streak (powder). The new mineral shows no fluorescence under UV (short and long wavelengths).

The main observed crystallographic forms are {010} and {001}. Twinning along the (100) plane is ubiquitous. Françoisite-(Ce) is brittle, with uneven fracture, and shows frequent cleavage along (010). Mohs hardness is ~3. Françoisite-(Ce) sinks in Clerici solution (thallium malonate and thallium formate), indicating a density in excess of 4.25 g/cm^3, in accordance with calculated density of 4.71 g/cm^3. This density was calculated from the empirical formula of the La Creusaz material (Table 1), assuming a water content of six H_2O and one hydroxyl group per formula unit, and a cell volume of 1831 Å^3 (unit cell refined from powder diffraction data; see below).

Optically, françoisite-(Ce) is biaxial negative. The maximum and minimum values of the refractive indices were measured using the immersion technique (elemental sulfur/diiodomethane solutions). The refractive indices of the liquids were checked using a Leitz-Jelley micro-refractometer with NaD at 24.5 °C. The measured extreme values are n_{min} = 1.740(1) and n_{max} = 1.750(1). Pleochroism is weak, X pale yellow, Y yellow. The average refractive index calculated using the Gladstone-Dale relationship is 1.750 for the average composition for the La Creusaz material in Table 1, normalized to an analytical total of 100 wt%. The constants from Mandarino (1976) and Piret and Deliens (1989) (for UO_3) were used. The calculated refractive index corresponds to a superior compatibility index $(1 - K_p/K_C) = 0.0061$ (Mandarino 1981).

Chemical composition

Chemical analyses of françoisite-(Ce) were carried out by means of an electron microprobe, and the results are summarized in Table 1. The following X-ray lines and analytical standards were used: U*M*α-uranium metal; Ca*K*α-wollastonite; Ba*L*α-barite; Pb*M*α-crocoite; Fe*K*α-hematite; Al*K*α-Al_2O_3; Y*L*α-YPO_4; La*L*α-$LaPO_4$; Ce*L*α-$CePO_4$; Pr*L*α-$PrPO_4$; Nd*L*α-$NdPO_4$; Sm*L*α-$SmPO_4$; Dy*L*α-$DyPO_4$; P*K*α-YPO_4; Si*K*α-wollastonite. The following additional elements were measured and found to be present at or below detection limit: Na_2O (≤0.07 wt%), MnO (<0.05 wt%), and SrO (<0.05 wt%). The Cameca SX50 microprobe was operated at 20 kV, 30 nA. Analyses were conducted using a tightly focused beam scanned over a surface of about 20 μm^2 to reduce beam damage due to dehydration, and data were corrected using the Cameca PAP routine (Pouchou and Pichior 1991).

Cerium is the dominant REE in all the grains analyzed (Fig. 2). High Si an Al values observed in analysis from Number 2 Workings, South Australia are related to micrometer scale inclusions of kaolinite, consequently, Si and Al were deducted and the analysis presented in Table 1. Minor amounts of Al in both analysis from La Creusaz and Number 2 Workings are consistent with classical substitution $Al^{3+} \leftrightarrow REE^{3+}$, and in the case of the phosphuranylite group, the Al term is represented by upalite, $Al[(UO_2)_3O(OH)(PO_4)_2]\cdot 7H_2O$.

Crystallography

Single-crystal X-ray studies could not be carried out because of lack of suitable crystals. The powder X-ray diffraction patterns of françoisite-(Ce) from both localities were collected by means of a Gandolfi camera (114.6 mm Gandolfi camera, Cu*K*α), and are similar to the pattern reported for françoisite-(Nd) by Piret et al. (1988). The unit-cell parameters for the françoisite-(Ce) from La Creusaz were refined from the powder data (Table 2), on the basis of françoisite-(Ce) being isostructural with françoisite-(Nd) (Piret et al. 1988). Françoisite-(Ce) is monoclinic, Z = 4, and probably shares space group $P2_1/c$ with françoisite-(Nd). The unit-cell dimensions refined from the powder data in Table 2 are a = 9.295(6), b = 15.53(2), c = 13.718(8) Å, β = 112.39(4)°, with V =

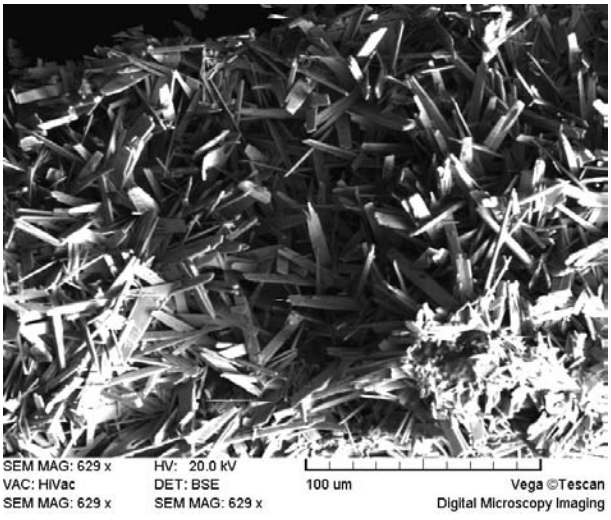

FIGURE 1. Scanning electron micrograph (backscattered electron mode) showing the morphology of the françoisite-(Ce) from La Creusaz.

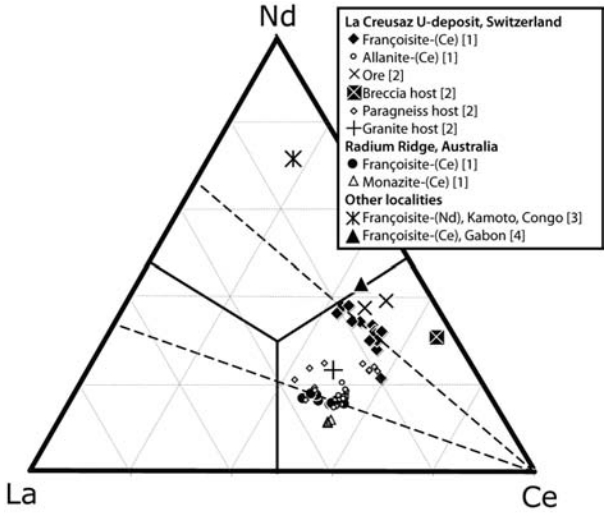

FIGURE 2. Triangular plot of the Nd, La, and Ce distribution (molar ratios) in françoisite-(Nd), and in françoisite-(Ce) and associated rocks and REE-bearing minerals at La Creusaz and Radium Ridge. Data sources: 1 = this study; 2 = Meisser (2003); 3 = Piret et al. (1988); 4 = Janeczek and Ewing (1996).

TABLE 1. Electron microprobe analyses of françoisite-(Ce) from La Creusaz and from Number 2 Workings

Mineral	La Creusaz, Switzerland				Number 2 Workings, Radium Ridge, South Australia*			
Sample	MGL no. 58321				MGL no. 79288			
n	8				5			
	mean	min	max	st.dev.	mean	min	max	st.dev.
Oxides (wt%)								
P_2O_5	10.16	9.60	10.62	0.37	9.36	8.99	9.82	0.30
SiO_2	0.48	0.23	0.82	0.20	3.41	1.64	4.64	1.21
Al_2O_3	0.42	0.14	0.89	0.22	3.62	1.98	4.80	1.05
UO_3	68.87	68.30	70.46	0.72	62.44	61.04	63.98	1.07
CaO	0.74	0.59	0.94	0.12	1.02	0.80	1.22	0.16
BaO	0.07	<0.05	0.24	0.08	0.28	0.17	0.54	0.15
PbO	1.61	1.04	2.33	0.48	0.27	0.12	0.51	0.15
FeO	0.03	<0.03	0.08	0.03	0.15	<0.03	0.59	0.25
Y_2O_3	0.49	0.31	0.63	0.11	0.08	0.03	0.15	0.05
La_2O_3	1.34	1.01	1.61	0.20	3.20	2.97	3.59	0.24
Ce_2O_3	3.76	3.19	4.46	0.48	4.64	4.24	5.15	0.44
Pr_2O_3	0.73	0.62	0.83	0.08	0.63	0.57	0.67	0.05
Nd_2O_3	2.79	2.33	3.11	0.26	1.62	1.48	1.71	0.09
Sm_2O_3	0.67	0.59	0.72	0.05	0.27	0.20	0.30	0.04
Dy_2O_3	0.06	<0.03	0.15	0.07	0.04	<0.03	0.10	0.05
H_2O_{calc}†	9.20	9.06	9.33	0.09	8.60	8.51	8.76	0.10
Sum	101.42			0.65	99.63			1.40
Atoms per formula unit								
P	1.82	1.75	1.89	0.05	1.80	1.72	1.85	0.05
Si	0.09	0.04	0.15	0.04	–	–	–	0.00
Al	0.11	0.03	0.22	0.05	0.31	0.21	0.40	0.09
Sum	2.02			0.08	2.11			0.06
U	3.06	3.01	3.13	0.04	2.97	2.94	2.99	0.02
Ca	0.17	0.13	0.22	0.03	0.25	0.19	0.30	0.04
Ba	0.01	<0.01	0.02	0.006	0.03	0.02	0.03	0.014
Pb	0.09	0.06	0.13	0.026	0.02	0.007	0.03	0.009
Fe	0.005	<0.005	0.014	0.005	0.03	<0.006	0.11	0.047
Y	0.05	0.04	0.07	0.012	0.01	0.004	0.02	0.007
La	0.10	0.08	0.12	0.015	0.27	0.25	0.30	0.019
Ce	0.29	0.25	0.35	0.039	0.38	0.35	0.42	0.033
Pr	0.06	0.05	0.06	0.006	0.052	0.047	0.055	0.003
Nd	0.21	0.18	0.23	0.019	0.13	0.12	0.14	0.007
Sm	0.05	0.04	0.05	0.004	0.021	0.015	0.023	0.003
Dy	0.004	<0.002	0.010	0.005	0.003	<0.003	0.007	0.004
Sum	1.04			0.04	1.20			0.06

Note: Normalization based on 15.5 oxygen equivalent pfu (Janeczek and Ewing 1996).
* Normalization assuming that all Si belongs to admixtures of kaolinite, $Al_2Si_2O_5(OH)_4$ (~25 mol% kaolinite).
† H_2O calculated assuming 13 H pfu (crystal structure of Piret et al. 1988).

TABLE 2. X-ray powder data for françoisite-(Ce) from La Creusaz, Switzerland

	d_{obs}	I_{meas}	d_{calc}	I_{calc}	h	k	l
1	9.88	5	9.82	11.8	0	$\bar{1}$	1
2	8.67	10	8.59	8.2	1	0	0
3	7.76	100	7.76	100	0	2	0
4	6.37	20	6.34	8.3	0	$\bar{0}$	2
5	5.77	60	5.76	27.9	1	$\bar{2}$	$\bar{0}$
6	4.94	5	4.94	8.2	1	$\bar{2}$	$\bar{2}$
7	4.78	5	4.79	8.7	0	$\bar{3}$	1
			4.47	8.2	$\bar{1}$	3	$\bar{1}$
			4.45	3.7	$\bar{2}$	1	1
8	4.42	30	4.43	10.4	$\bar{2}$	0	2
9	4.37	30	4.36	16.5	1	0	$\bar{2}$
			4.36	4	1	1	$\bar{3}$
10	3.87	60	3.88	25.1	$\bar{0}$	4	0
			3.84	11.1	$\bar{2}$	2	2
11	3.43	70	3.43	22.8	$\bar{1}$	$\bar{0}$	4
12	3.31	10	3.31	8.6	0	$\bar{4}$	$\bar{2}$
13	3.14	80	3.14	34.6	1	2	$\bar{4}$
14	3.08	5	3.09	16	3	0	$\bar{2}$
15	3.06	5	3.05	15	2	$\bar{0}$	2
16	2.974	5	2.989	4.8	2	$\bar{3}$	1
	–		2.899	9.2	1	$\bar{4}$	2
17	2.871	30	2.870	25	$\bar{3}$	$\bar{2}$	2
18	2.844	30	2.841	22.6	$\bar{2}$	$\bar{2}$	2
19	2.633	5	2.638	0.9	$\bar{2}$	1	5
			2.630	2.8	$\bar{3}$	3	$\bar{1}$
20	2.564	20	2.569	6.4	$\bar{1}$	4	$\bar{4}$
			2.562	2.8	$\bar{1}$	$\bar{5}$	3
21	2.398	10	2.399	3.6	$\bar{2}$	$\bar{4}$	2
			2.397	4.1	$\bar{1}$	6	$\bar{2}$
22	2.392	10	2.394	1.2	$\bar{0}$	6	$\bar{2}$
23	2.183	5	2.184	1.1	$\bar{3}$	3	$\bar{5}$
			2.183	1.9	$\bar{0}$	7	$\bar{1}$
24	2.139	5	2.138	1.1	$\bar{3}$	5	3
25	2.065	5	2.069	10.7	$\bar{4}$	2	$\bar{0}$
			2.064	5.9	1	6	$\bar{4}$
26	2.038	40	2.038	7.1	$\bar{0}$	2	$\bar{6}$
27	1.973	10	1.973	0.4	$\bar{3}$	$\bar{6}$	1
			1.973	3.5	$\bar{2}$	$\bar{6}$	2
28	1.916	10	1.916	6.6	$\bar{4}$	0	6
29	1.892	20	1.890	6.5	1	0	$\bar{6}$
30	1.861	10	1.860	5.4	4	2	$\bar{6}$
31	1.831	10	1.832	2.1	5	0	$\bar{4}$
32	1.801	5	1.808	2.2	$\bar{3}$	0	4
33	1.781	5	1.783	2.3	$\bar{5}$	$\bar{2}$	4
			1.782	1.7	4	$\bar{2}$	2
34	1.762	5	1.760	2.4	$\bar{3}$	2	4
35	1.717	5	1.718	4.7	$\bar{4}$	4	6
			1.717	2.7	5	$\bar{0}$	0
36	1.702	20	1.699	4.1	1	$\bar{4}$	$\bar{6}$
37	1.672	5	1.674	5.8	$\bar{2}$	2	$\bar{8}$
38	1.65	10	1.656	2.4	$\bar{5}$	4	4
			1.652	2.2	$\bar{4}$	6	0
39	1.568	5	1.570	1.5	$\bar{5}$	4	$\bar{0}$
			1.568	1.9	2	$\bar{4}$	$\bar{8}$
			1.567	3.4	1	$\bar{8}$	$\bar{4}$
40	1.544	10	1.545	1.9	6	0	$\bar{4}$

Notes: Gandolfi camera, 114.6 mm diameter, Cu*K*α/Ni-filtered, 40 kV, 30 mA, 100 h exposure time. Estimated reading errors of ±0.15 mm, leading to following errors on *d*-values: 9.88(8), 2.038(3), 1.544(2) Å.

1831(3) Å^3. In comparison, the type specimen of françoisite-(Nd) had a = 9.298(2), b = 15.605(4), c = 13.668(2) Å, β = 112.77(1)°, with V = 1828.6(7) Å^3 (Piret et al. 1988).

Relation to other species and comments on genesis

Françoisite-(Ce) is the Ce-dominant analog of françoisite-(Nd) (Piret et al. 1988). The two species are structurally related to the phosphuranyllite group (Burns 1999). At the type locality (Kamoto, RDC), Françoisite-(Nd) occurs directly on weathered uraninite, and Nd is clearly the dominant REE (Ce/Nd = 0.22; Fig. 2; Table 3). A françoisite-(Ce) with nearly equal amounts of Ce and Nd (Ce_2O_3 3.25–3.58 wt%; Nd_2O_3 3.61–3.66 wt%; Ce/Nd = 1.01) has been reported from the oxidation zone of the Bangombé natural fission reactor, Gabon, by Janeczek and Ewing (1996).

A triangular plot of the three main REE present in françoisite-(REE) (Fig. 2) shows that françoisite-(Ce) is characterized by nearly constant La/Nd ratios at La Creusaz [0.51(0.05); see Table 3] and Radium Ridge [1.98(11)], but both localities display a range in Ce concentrations. All analyses of françoisite from La Creusaz and Radium Ridge are Ce-dominant, with a few analyses from La Creusaz approaching Nd/Ce = 1 (Fig. 2).

The controls on REE composition of minerals precipitating from solutions are complex, depending under equilibrium conditions upon the crystallographic control exerted by the mineral, the REE composition of the fluid, the pressure and temperature, and the aqueous speciation of the REE (i.e. nature of the stable complexes, which itself depends upon the ligands present in solution, pH, and redox) (Lipin and McKay 1989; review of REE partitioning between minerals and fluids in Brugger et al. 2008).

In chondritic meteorites and in post-Archaean shales, Ce is the most abundant REE, followed by Nd or La (0.638, 0.474,

and 0.245 ppm, respectively, in chondrites; Evensen et al. 1978; 79.6, 33.90, and 38.2 ppm in post-Archaean Australian Shales; McLennan 1989). The crystallization of minerals in which Nd or La are the dominant REE usually occurs in the weathering environment, under conditions where Ce^{4+} becomes stable. Ce^{4+} is highly insoluble, usually coprecipitating with Fe and Mn-oxyhydroxides (e.g., Takahashi et al. 2000); hence Ce tends to be immobile where Ce^{4+} is present. Taunton et al. (2000) show how this behavior results in preferential leaching of trivalent REE in the top of the weathering profile in a granite, resulting in a top soil enriched in Ce relative to the fresh granite, and in soil solutions depleted in Ce relative to the other REE. This process can lead to the formation of unusual Nd- and La-rich minerals during the weathering of REE-rich ore deposits (e.g., Brugger et al. 2006a; Pring et al. 2006), and it is probably responsible for the Nd-rich and Ce-poor composition of françoisite-(Nd) at Kamoto. Figure 2 reveals that some small-scale fractionation of Ce relative to the other REE happened at both La Creusaz and Radium Ridge, although Ce remains the main REE in all analyzed samples from these localities. This hints that REE transport occurred under near-surface oxidizing conditions, but that only a small proportion of Ce was oxidized to Ce^{4+} along the path of REE aqueous transport.

At Radium Ridge, the uraniferous ore is characterized by large quantities of monazite-(Ce). Assuming that this monazite-(Ce) is the source of REE in françoisite-(Ce), the La/Nd ratio in françoisite-(Ce) appears to be ~1.5 times that in the "source" monazite-(Ce) (Fig. 2; Table 3). At La Creusaz, allanite-(Ce) resulting from the destabilization of monazite-(Ce) under metamorphic conditions (see Fig. 3) is the most likely source of REE in françoisite-(Ce). According to Negga et al. (1986) and Finger et al. (1998), the necessary amounts of Ca, Fe, Si, and Al for the breakdown of monazite-(Ce) could be simply supplied by a fluid phase chemically buffered through other metamorphic reactions involving the main mineral components of the rock (e.g. plagioclase- and biotite-group minerals). Françoisite-(Ce) from La Creusaz is the result of the interaction between meteoritic fluids charged in REE and PO_4^{3+} via alteration of a pyrite-fluorapatite-allanite-(Ce) gneiss assemblage (see Fig. 3) with uraninite hosted in uraninite-pyrite-quartz vein.

The La/Nd ratio decreases from 1.78 in allanite-(Ce) to 0.51 in françoisite-(Ce) at La Creusaz, and from 2.97 in monazite-(Ce) to 1.98 in françoisite-(Ce) at Radium Ridge (Table 3). Crystallographic control of REE uptake by françoisite-(Ce) is expected to favor light REE such as La over Nd, and hence is not likely to explain the observed fractionation trend. Instead, the observed fractionation of the La/Nd ratio between source mineral and françoisite-(Ce) most probably reflects enhanced mobility of heavier REE relative of lighter REE, due do stronger stability of the aqueous complexes involved. Brugger et al. (2005) provide a chemical analysis of a modern, U-rich (665 ppb) groundwater from metasomatic rocks similar to that hosting the Number 2 workings orebody ("Radium Creek Bore" sample). Thermodynamic calculations performed using Geochemist's Workbench (Bethke 2008) and the thermodynamic properties in a customized version of the Lawrence Livermore National Laboratory database (Version 8; Revision 7) suggest that U exists mainly as

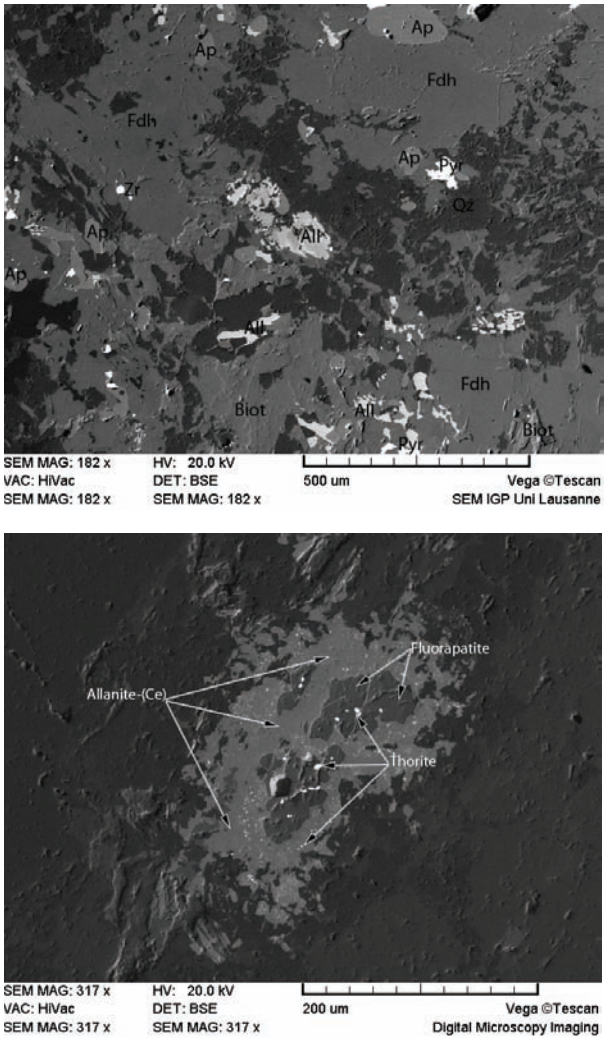

FIGURE 3. Primary light REE-bearing mineral assemblage in paragneisses from La Creusaz, on which françoisite-(Ce) developed. (**top**) Allanite-(Ce) rich zone. (**bottom**) Detail showing assemblage of allanite-(Ce), fluorapatite, and thorite, resulting from the metamorphic destabilization of monazite-(Ce). Abbreviations: All = allanite-(Ce); Ap = fluorapatite; Biot = Biotite-group mica; Fdh = K-feldspar; Pyr = pyrite; Qz = quartz; Zr = zircon.

TABLE 3. Atomic ratio for the rare earth element composition of françoisite-(REE) and possible REE sources

Mineral/rock	Ce/Nd (atomic ratio)	La/Nd (atomic ratio)	Ce/(La+Nd) (atomic ratio)
Françoisite-(Nd), Kamoto, RDC (Piret et al. 1988)	0.22	0.16	0.19
Françoisite-(Ce), Bangombé, Gabon (Janeczek and Ewing 1996)	1.01	0.28	0.79
Françoisite-(Ce), La Creusaz (n = 13) *	1.5(3) range 1.12–1.93	0.51(5) range 0.43–0.60	1.0(2) range 0.74–1.21
Allanite-(Ce), La Creusaz (n = 22)	3.1(2)	1.7(2)	1.13(4)
Françoisite-(Ce), Radium Ridge (n = 8)	3.0(3) range 2.53–3.40	2.0(1) range 1.86–2.17	1.0(1) range 0.83–1.19
Monazite-(Ce), Radium Ridge (n = 3)	4.6(1)	3.0(1)	1.15(1)

* One outlier analysis (with Ce/Nd = 2.71) was omitted.

a uranyl carbonate complex ($REECO_3^+$) in these waters assuming a dissolved phosphate contents of 10 ppm, and as a phosphate complex [$REEPO_4$(aq)] at a higher phosphate concentration of 100 ppm. Based on the dissociation constants listed in Spahiu and Bruno (1995; REE phosphate complexes) and Haas et al. (1995; REE carbonates), the activity ratios among La:Ce:Nd will be 1:1.92:3.85 for $REECO_3^+$ and 1:2.45:7.14. These calculations hence confirm that carbonate and phosphate complexes become increasingly stronger with increasing atomic number of the REE, favoring transport of Nd over Ce and La; this can explain the fractionation trend observed at Radium Ridge and La Creusaz.

In conclusion, françoisite-(REE) documents small-scale mobility of uranyl and REE during the weathering of U-rich mineralization. Françoisite-(REE) offers a natural analog for understanding element mobility around high level radioactive waste, that can contain fissiogenic REE, and may include phosphate-bearing chemical barriers (e.g., Jensen et al. 2002; Miller et al. 2000; Hidaka et al. 2005).

ACKNOWLEDGMENTS

We are grateful to Pierre Vonlanthen and Peter O. Baumgartner (SEM/EDXS laboratory, Institute of Geology and Paleontology, UNIL, Lausanne) for the help with the SEM facilities. The manuscript benefited from the insightful comments of Janusz Janeczek and an anonymous reviewer. This is TRaX publication no. 90.

REFERENCES CITED

Bakker, R.J. and Elburg, M.A. (2006) A magmatic-hydrothermal transition in Arkaroola (northern Flinders Ranges, South Australia): From diopside-titanite pegmatites to hematite-quartz growth. Contributions to Mineralogy and Petrology, 152, 541–569.

Bethke, C.M. (2008) Geochemical and Biogeochemical Reaction Modeling (second edition), 564 p. Cambridge University Press, New York.

Brugger, J., Burns, P., and Meisser, N. (2003a) Contribution to the mineralogy of acid drainage of uranium minerals: Marécottite and the zippeite-group. American Mineralogist, 88, 676–685.

Brugger, J., Ansermet, S., and Pring, A. (2003b) Uranium minerals from Mt. Painter, Northern Flinders Ranges, South Australia. Australian Journal of Mineralogy, 9/1, 15–31.

Brugger, J., Krivovichev, S.V., Berlepsch, P., Meisser, N., Ansermet, S., and Armbruster, T. (2004) Spriggite, $Pb_3[(UO_2)_6O_8(OH)_2](H_2O)_3$, a new mineral with β-U_3O_8-type sheets: Description and crystal structure. American Mineralogist, 89, 339–347.

Brugger, J., Long, N., McPhail, D.C., and Plimer, I. (2005) An active amagmatic hydrothermal system: The Paralana hot springs, Northern Flinders Ranges, South Australia. Chemical Geology, 222, 35–64.

Brugger, J., Ogierman, J., Pring, A., Waldron, H., and Kolitsch, U. (2006a) Origin of the secondary REE-minerals at the Paratoo copper deposit near Yunta, South Australia. Mineralogical Magazine, 70, 609–627.

Brugger, J., Wallwork, K.S., Meisser N., Pring, A., Ondruš, P., and Čejka, J. (2006b) Pseudojohannite from Jáchymov, Musonoï, and La Creusaz: A new member of the zippeite-group. American Mineralogist, 91, 929–936.

Brugger, J., Etschmann, B., Pownceby, M., Liu, W.H., Grundler, P., and Brewe, D. (2008) Oxidation state of europium in scheelite: Tracking fluid-rock interaction in gold deposits. Chemical Geology, 257, 26–33.

Burns, P. (1999) The crystal chemistry of uranium. In P.C. Burns and R. Finch, Eds., Uranium: Mineralogy, geochemistry, and the environment, 38, p. 23–90. Reviews in Mineralogy, Mineralogical Society of America, Chantilly, Virginia.

Coats, R.P. and Blissett, A.H. (1971) Regional and economic geology of the Mount Painter province. Department of Mines, Geological Survey of South Australia, Bulletin 43, 426 p.

Drexel, J.F. and Major, R.B. (1990) Mount Painter uranium-rare earth deposits. In F.E. Hughes, Ed., Geology of the Mineral Deposits of Australia and Papua New Guinea. Australasian Institute of Mining and Metallurgy, Melbourne.

Drexel, J.F., Preiss, W.V., and Parker, A.J. (1993) The geology of South Australia. Volume 1: The Precambrian. Geological Survey of South Australia, Bulletin 54, 242 p.

Elburg, M., Bons, P., Foden, J., and Brugger, J. (2003) A newly defined Late Ordovician magmatic-thermal event in the Mt. Painter Province, northern Flinders Ranges, South Australia. Australian Journal of Earth Sciences, 50, 611–631.

Evensen, N.M., Hamilton, P.J., and O'Nions, R.K. (1978) Rare-earth abundances in chondritic meteorites. Geochimica et Cosmochimica Acta, 42, 1199–1212.

Fanning, C.M., Teale, G.S., and Robertson, R.S. (2003) Is there a Willyama Supergroup sequence in the Mount Painter Inlier? In M. Peljo, Ed., Broken Hill Exploration Initiative, p. 38–41. Geoscience Australia, Broken Hill, Australia.

Finger, F., Broska, I., Roberts, M.P., and Schermaier, A. (1998) Replacement of primary monazite by apatite-allanite-epidote coronas in an amphibolite facies granite gneiss from eastern Alps. American Mineralogist, 83, 248–258.

Gilliéron, F. (1988) Zur Geologie der Uranmineralisation in den Schweizer Alpen. Beiträge zur Geologie der Schweiz, Geotechnische Serie, 77, 54 p.

Haas, J.R., Shock, E.L., and Sassani, D.C. (1995) Rare earth elements in hydrothermal systems: estimates of standard partial molal thermodynamic properties of aqueous complexes of the rare earth elements at high pressures and temperatures. Geochimica et Cosmochimica Acta, 59, 4329–4350.

Hidaka, H., Janeczek, J., Skomurski, F.N., Ewing, R.C., and Gauthier-Lafaye, F. (2005) Geochemical fixation of rare earth elements into secondary minerals in sandstones beneath a natural fission reactor at Bangombé, Gabon. Geochemica et Cosmochemica Acta, 69, 685–694.

Idnurm, M. and Heinrich, C.A. (1993) A paleomagnetic study of hydrothermal activity and uranium mineralization at Mt. Painter, South Australia. Australian Journal of Earth Sciences, 40, 87–101.

Janeczek, J. and Ewing, R.C. (1996) Phosphatian coffinite with rare earth elements and Ce-rich françoisite-(Nd) from sandstone beneath natural fission reactor at Bangombé, Gabon. Mineralogical Magazine, 60, 665–669.

Jensen, K.A., Palenik, C.S., and Ewing, R.C. (2002) U^{6+} phases in the weathering zone of the Bangombé U-deposit: Observed and predicted mineralogy. Radiochimica Acta, 90, 1–9.

Levinson, A.A. (1966) A system of nomenclature for rare-earth minerals. American Mineralogist, 51, 152–158.

Lipin, B.R. and McKay, G.A. (1989) Geochemistry and Mineralogy of Rare Earth Elements, 21, 348 p. Reviews in Mineralogy, Mineralogical Society of America, Chantilly, Virginia.

Mandarino, J.A. (1976) The Gladstone-Dale relationship. Part I: Derivation of new constants. Canadian Mineralogist, 14, 498–502.

——— (1981) The Gladstone-Dale relationship. Part IV: The compatibility concept and its application. Canadian Mineralogist, 19, 441–450.

McLennan, S.M. (1989) Rare earth elements in sedimentary rocks: influence of provenance and sedimentary processes. In B.R. Lipin and G.A. McKay, Eds., Geochemistry and Mineralogy of Rare Earth Elements, 21, p. 169–200. Reviews in Mineralogy, Mineralogical Society of America, Chantilly, Virginia.

Meisser, N. (2003) La minéralogie de l'uranium dans le massif des Aiguilles Rouges (Alpes occidentales). Ph.D. thesis, Université de Lausanne, Switzerland, 255 p.

Miller, W., Alexander, R., Chapman, N., McKinley, I., and Smellie, J. (2000) Geological Disposal of Radioactive Wastes and Natural Analogues, 328 p. Pergamon, Amsterdam.

Negga, H.S., Sheppard, S.M.F., Rosenbaum, J.M., and Cuney, M. (1986) Late Hercynian U-vein mineralization in the Alps; fluid inclusion and C, O, H isotopic evidence for mixing between two externally derived fluids. Contributions to Mineralogy and Petrology, 93/2, 179–186.

Neumann, N., Sandiford, M., and Foden, J. (2000) Regional geochemistry and continental heat flow: implications for the origin of the South Australian heat flow anomaly. Earth and Planetary Science Letters, 183, 107–120.

Piret, P. and Deliens, M. (1989) The Gladstone-Dale constant $k(UO_3)$ for uranyl phosphates and arsenates. Canadian Mineralogist, 27, 533–534.

Piret, P., Deliens, M., and Piret-Meunier, J. (1988) La françoisite-(Nd), nouveau phosphate d'uranyle et de terres rares; propriétés et structure cristalline. Bulletin de Minéralogie, 111, 443–449.

Pring, A., Wallwork, K., Brugger, J., and Kolitsch, U. (2006) Paratooite-(La), a new lanthanum-dominant rare-earth copper carbonate from Paratoo, South Australia. Mineralogical Magazine, 70, 131–138.

Pouchou, J. and Pichior, F. (1991) Quantitative analysis of homogeneous or stratified microvolumes applying the model "PAP." In K.F.J. Heinrich and D.E. Newbury, Eds., Electron Probe Quantitation, p. 31–75. Plenum, New York.

Sandiford, M., Hand, M., and McLaren, S. (1998) High geothermal gradient metamorphism during thermal subsidence. Earth and Planetary Science Letters, 163, 149–165.

Spahiu, K. and Bruno, J. (1995) A selected thermodynamic database for REE to be used in HLNW performance assessment exercises. SKB Technical Report, 95-35, 80 p.

Takahashi, Y., Shimizu, H., Usui, A., Kagi, H., and Nomura, M. (2000) Direct observation of tetravalent cerium in ferromanganese nodules and crusts by X-ray-absorption near-edge structure (XANES). Geochimica et Cosmochimica Acta, 64, 2929–2935.

Taunton, A.E., Welch, S.A., and Banfield, J.F. (2000) Microbial controls on phosphate and lanthanide distributions during granite weathering and soil formation. Chemical Geology, 169, 371–382.

MANUSCRIPT RECEIVED OCTOBER 1, 2009
MANUSCRIPT ACCEPTED MAY 18, 2010
MANUSCRIPT HANDLED BY ANTON CHAKHMOURADIAN